Korean J. Chem. Eng., 39(3), 684-694 (2022)
DOI: 10.1007/s11814-021-0928-8

pISSN: 0256-1115
eISSN: 1975-7220

Cellulose-type binder enabling $CuCl_2$ supported on nanoporous bayerite to have high CO adsorption ability via reduction of Cu^{2+} to Cu^+

Jungsu Kim*,,‡, Kanghee Cho*,‡, Taesung Jung*, Hee Tae Beum*,
Jong-ho Park*, Young Woo Rhee**,†, and Sang Sup Han*,†**

*Climate Change Research Division, Korea Institute of Energy Research, 152 Gajeong-ro, Yuseong-gu, Daejeon 34129, Korea
**Graduate School of Energy Science and Technology, Chungnam National University,
99 Daehak-ro, Yuseong-gu, Daejeon 34134, Korea

(*Received 30 March 2021 • Revised 13 July 2021 • Accepted 13 August 2021*)

Abstract−Previously, we developed a powder-form nanoporous CO-selective adsorbent synthesized via thermal monolayer dispersion of CuCl on bayerite, showing high CO adsorption capacity (48.5 cm^3g^{-1}) and a high CO/CO_2 selectivity (12.4). For its industrial applications, it is necessary to pelletize it, avoiding pressure-drop problems. Here, we demonstrate a facile three-step method of pelletizing a CuCl/bayerite: 1) physical mixing of CuCl, methyl-cellulose, inorganic-binder, and bayerite, 2) pelletizing, and 3) thermal treatment at 573 K under vacuum. The pelletized adsorbent shows high CO adsorption capacity (42 cm^3g^{-1}), CO/CO_2 selectivity (12), and commercial-level mechanical strength (1.3 kg_f). Notably, the added methyl-cellulose binder has reducing role that maintains the initial CO adsorption capacity for 100 days' exposure to humid air-condition, although CuCl-based adsorbent easily lost CO adsorption ability owing to oxidation of Cu^+ to Cu^{2+}. $CuCl_2$, showing no specific interaction with CO, was converted to Cu^+ by the methyl-cellulose. Thus, adsorbent prepared using $CuCl_2$ instead of CuCl with the methyl-cellulose also showed high CO adsorption capacity (31.6 cm^3 g^{-1}) and maintained the initial capacity after seven days' exposure. The reducing role of the methyl-cellulose binder allows inexpensive and feasible synthesis of the CO-adsorbent using $CuCl_2$ that can be easily dispersed on bayerite, without additional reduction treatment.

Keywords: CO-selective Adsorption, CuCl, Bayerite, Methyl Cellulose, Reducing Agent

INTRODUCTION

Carbon monoxide (CO) is generated from various industries and chemical processes such as steel-making, steam-methane-reforming (SMR), and partial-oxidation (POX) [1-3]. CO is highly toxic to humans and a poisoning impurity in end-user applications such as fuel cells that use hydrogen generated from the SMR process [2,4], which is normally removed via an additional combustion process before emission [5]. However, carbon monoxide can be used as a highly valuable starting material of various chemical products such as syn gas ($CO+H_2$), polyurethane, polycarbonate, formic acid, acetic acid, and isocyanates [1,6,7], when it is selectively separated from the aforementioned sources containing impurities (*e.g.*, CO_2, H_2, N_2, and CH_4, as well as CO).

For the selective separation of carbon monoxide, cryogenic distillation, absorption-based processes, and adsorption-based processes are generally used [6,8-12]. Cryogenic distillation is the most generally applied method and is suitable for large-scale separation, but it is highly energy-consuming, especially in the case of separation between carbon monoxide and nitrogen, which have similar boiling points [11]. The COSORB process is a commercial process based on CO absorption that affords high CO purity and high yield, but this process uses an expensive and toxic absorbent, $CuAlCl_4$/toluene solution [8].

In the adsorption process, which allows less expensive, energy-saving, and medium-scale separation of carbon monoxide, nanoporous adsorbents containing transition metal cations such as Ag(I) and Cu(I) that exhibit strong interaction with CO molecules via π-complexation and π back-bonding are normally used [9,13-19]. In this process, CO selectivity against other impurities such as CO_2, H_2, N_2, and CH_4 is a key factor to decide the process performance such as the recovery rate and the productivity of CO product. In the 1990s, Xie et al. synthesized a CO-selective adsorbent by impregnating CuCl on zeolite Y via thermal monolayer dispersion, and opened the adsorption-based CO separation field [20]. This adsorbent exhibited CO adsorption capacity higher than 2.2 mmol g^{-1} at 298 K but showed similarly high CO_2 adsorption capacity.

According to previous reports and our preceding research, the selection of supporting materials used for dispersing the CuCl component is important to obtain high selectivity of CO [21,22]. To date, various nanoporous materials such as activated carbon, silica gel, mesoporous silica (e.g., MCM-41, SBA-15, etc.), and mesoporous alumina have been tested to synthesize highly CO-selective adsorbents [23-29]. Recently, our research group synthesized CO adsorbents by dispersing CuCl on boehmite and bayerite, which are precursor materials of mesoporous alumina, via the TMD method [21,22]. CuCl/boehmite exhibited 35 cm^3 g^{-1} (STP)

[†] To whom correspondence should be addressed.
E-mail: ywrhee@cnu.ac.kr, sshan@kier.re.kr
[‡] Both authors contributed equally to this work with first authorship.

CO adsorption capacity at 293 K and a 12.4 CO/CO_2 separation factor. CuCl/bayerite exhibited somewhat higher CO adsorption capacity (48.5 cm^3 g^{-1}, STP) due to its larger surface area (469 m^2 g^{-1}) and a CO/CO_2 separation factor of 16.8. In addition, it exhibited high CO selectivity against N_2, CH_4, and H_2. We confirmed that bench-scale CO-VPSA (vacuum-pressure swing adsorption) process using the CuCl/boehmite adsorbent provides high CO productivity and recovery rate (details are not reported here, due to a non-disclosure agreement with a company that made a technology transfer with our institute). This process also shows strong potential for industrialization.

However, prior to the industrialization of CO-VPSA using our CO-selective adsorbents, it is necessary to resolve two significant issues related to the adsorbent. The first is to pelletize the CuCl/boehmite and CuCl/bayerite adsorbents in powder form. Using the adsorbents in powder form in an industrial VPSA process causes a critical pressure drop problem. In typical applications of separation processes, an adsorbent in a sphere-type or rod-type form with sufficient mechanical strength is used (normally higher than 1.0 kg_f). To pelletize powder-form CO adsorbents with quite uniform size, systematic research and technical know-how such as the selection of suitable binder, uniform mixing of the adsorbent and the binder species, and uniform extrusion are required. The pelletization of the powder-form adsorbent is not simple technical work and is based on science.

The second is to avoid oxidation of CuCl species dispersed on boehmite and bayerite. Cu^+ species in a CuCl molecule is easily oxidized to Cu^{2+} by water vapor and oxygen present in the atmosphere, and Cu^{2+} has no specific interaction with CO molecules [30-32]. In particular, as the CuCl component is highly dispersed on boehmite and bayerite of nanometer size, the rate of oxidation increases significantly. We confirmed that the CuCl/boehmite and CuCl/bayerite lost CO adsorption ability considerably after exposing the adsorbents to humid atmospheric conditions for a day. In a previous work, Jin et al. added a $FeCl_2$ component as a sacrificial oxidant to avoid the oxidation of CuCl [33]. However, in our cases of CuCl/boehmite and CuCl/bayerite, the addition of $FeCl_2$ was not sufficiently effective to reduce the oxidation rate of CuCl, but rather it reduced the adsorption capacity of CO.

In this work, we proposed a new concept of pelletizing a CuCl/bayerite adsorbent to a spherical shape while providing sufficiently high mechanical strength. Methyl cellulose was used as the main binder species and a small amount of alumina-type inorganic binder was added to increase the mechanical strength. In the typical pelletization method of a commercial adsorbent, an alumina- (or silica-) type inorganic binder is used as the main binder, while an organic species such as methyl cellulose is used as a plasticizer and a macropore-generating agent that is thermally calcined. Notably, we confirmed that the methyl cellulose that is used as the main binder species in this work strongly acts as a reducing agent to maintain the oxidation state of Cu(I) and the initial CO adsorption capacity for several months.

In our proposed method, it is noteworthy that the thermal dispersion of CuCl on the bayerite material, the pelletization of the powder adsorbent, and the generation of a reducing agent for maintaining the CO adsorption capacity occur simultaneously. The CuCl/bayerite pellet with quite uniform size was formed via the following steps: 1) physical mixing of cellulose, inorganic binder species, CuCl, and bayerite, 2) preparing an extrudate-friendly dough of the mixture, 3) pelletizing, and 4) thermal treatment under a vacuum condition. To find the optimum conditions of the pelletization, various types of organic binders such as methyl cellulose, carboxy methyl cellulose, propyl methyl cellulose, hydroxypropyl methyl cellulose, and starch were tested. In particular, the methyl cellulose was tested by varying the amount used. The possibility of decomposition and structural change of the organic binder species during the thermal treatment was confirmed by thermogravimetric (TG) and FT-IR analyses. The mechanical strength of the pelletized adsorbent was also measured. To evaluate the CO adsorption capacity and CO selectivity of the pelletized CuCl/bayerite adsorbent, adsorption isotherms of the adsorbent for CO, CO_2, CH_4, N_2, O_2, and H_2 were measured at 293 K. In addition, to confirm the oxidation resistance of the pelletized adsorbent, the adsorption isotherms of CO were measured again after the adsorbent was exposed to a humid air condition for at least seven days.

To verify the reducing ability of the organic binder species to CuCl species, we applied the methyl cellulose to $CuCl_2$/bayerite synthesized by the impregnation of $CuCl_2$, which is a further oxidized state of CuCl and shows no adsorption capacity to CO species. We then measured the CO adsorption isotherm after thermal treatment of the mixture of methyl cellulose and $CuCl_2$/bayerite adsorbent. The conversion of Cu(II) to Cu(I) by the reduction role of methyl cellulose was confirmed by X-ray photoelectron spectroscopy (XPS) measurement.

EXPERIMENTAL

1. Reagents

CuCl (97%) was purchased from Sigma Aldrich. $CuCl_2 \cdot 2H_2O$ (97%) was purchased from Samchun Chemicals. Methyl cellulose (MC), carboxy methyl cellulose (CMC), propyl methyl cellulose (PMC), hydroxyl propyl methyl cellulose (HMC), and starch that were tested as organic binder species in this work were commercial products.

2. Preparation of Pellet-type Adsorbent

The pelletization and thermal monolayer dispersion (TMD) of CuCl on bayerite material were performed at once. Prior to the pelletization and TMD process, raw bayerite material was activated by thermal treatment at 623 K (ramping rate=1 K min^{-1}) under nitrogen flow (flow rate=100 cm^3 min^{-1}) for 6 h, in order to increase the BET surface area of the bayerite material. The activated bayerite, CuCl, small amount of inorganic binder, and one type of cellulose derivatives (MC, CMC, PMC, HMC, and starch) were physically mixed with composition of 6.4 bayerite: 3.6 CuCl, 1 inorganic binder: 0.2-1.4 cellulose in weight ratio. With continuous addition of distilled water with optimum amount, we made elastic dough of the reagent mixture. This reagent mixture dough was extruded by high-pressure screw to be rod-shape pellets. The reagent mixture in pellet form was dried at 333 K under vacuum condition for 3 h, and it was heated to 573 K for 12 h for TMD of CuCl.

To confirm the reducing ability of MC species, we also synthesized $CuCl_2$/bayerite pellet adsorbent with the addition of MC. The activated bayerite, $CuCl_2 \cdot 2H_2O$, inorganic binder, and MC were physically mixed with composition of 6.4 bayerite: 3.6 $CuCl_2 \cdot 2H_2O$, 1 inorganic binder: 1 MC in weight ratio. Following procedures are same as the CuCl/bayerite pellet was synthesized.

3. Physico-chemical Characterization

TA Instruments Q 50 was used to measure TG/DTG curves of cellulose species. The weight of cellulose sample was monitored during heating the sample to 573 K with 1 K min^{-1} of ramping rate under nitrogen flow (flow rate=70 cm^3 min^{-1}) and consequently holding the final temperature for 16 h. FT-IR spectra of the thermally treated cellulose derivatives were measured using VERTEX 80v equipped with DTGS detector in the frequency range of 500-4,000 cm^{-1} under air at room temperature. The structure of the adsorbents was determined by powder XRD (Rigaku, D/MAX-2500) using Cu Kα radiation with a 0.02° step width and 1 s step time. The morphology and the elemental distribution of the adsorbent were characterized by SEM equipped with EDS (Hitachi, S-4800). Nitrogen sorption isotherm was taken at 77 K using volumetric sorption analyzer (3Flex, Micromeritics). Prior to the measurement, the adsorbent samples were degassed at 573 K under vacuum for 6 h to remove the adsorbed water or VOC components. XPS spectra of various CuCl/bayerite pellet samples were obtained using MultiLab 2000 (Thermo Scientific, Al Kα radiation). Adsorption isotherms of CO, CO_2, O_2, N_2, H_2, and CH_4 were measured by using volumetric analyzer (Tristar 3020, Micromeritics) at 293 K. Prior to the measurement, the adsorbent samples were degassed at 573 K under vacuum for 6 h. Adsorption separation factor was calculated from the ratios of the adsorption amounts of CO to those of other impurities at 101 kPa.

RESULTS AND DISCUSSION

1. Synthesis of CuCl/Bayerite in Pellet Form

In our previous report [22] we synthesized a CO-selective adsorbent in powder form by dispersing CuCl on bayerite via a thermal monolayer dispersion (TMD) step. We used only CuCl and bayerite component but no inorganic binder or organic binder species. To find the synthesis conditions of CuCl/bayerite adsorbent that maximize the CO adsorption capacity and CO selectivity, the ratio of CuCl to bayerite and the TMD temperature were varied. In this report, the adsorbent exhibited the highest CO adsorption capacity (48.5 cm^3 g^{-1} at 293 K) when 30 wt% of CuCl was dispersed on bayerite at 573 K. When 36 wt% of CuCl was dispersed on bayerite, the synthesized adsorbent exhibited CO adsorption capacity of 41.6 cm^3 g^{-1} and the highest CO/CO_2 separation factor (35.5).

In this work, we synthesized a CuCl/bayerite-type CO-selective adsorbent in pellet form via a simple method using a cellulose-type organic species as the main binder and an alumina-type inorganic binder additive for enhancing the mechanical strength of the adsorbent pellet. The CuCl/bayerite pellet with quite uniform size was formed via the following steps: 1) physical mixing of methyl cellulose, inorganic binder species, CuCl, and bayerite, 2) making an extrudate-friendly dough of the mixture, 3) pelletizing, and 4) thermal treatment at 573 K under a vacuum condition (see Fig. 1). We confirmed that the cellulose-type organic species acts as a strong binder to form a pellet of CuCl/bayerite adsorbent while simultaneously acting as a reducing agent to maintain the oxidation state of CuCl and the initial CO adsorption capacity of the adsorbent for several months. We explain the details of the reducing role of the cellulose species in Section 3.5.

2. Transformation of Cellulose Species at TMD Temperature

As mentioned, a cellulose-type organic species was used as the main binder to make the CuCl/bayerite adsorbent in pellet form. Various types of cellulose derivatives, methyl cellulose (MC), carboxy methyl cellulose (CMC), propyl methyl cellulose (PMC), hydroxyl propyl methyl cellulose (HMC), and starch were tested as organic binder species to form the CuCl/bayerite pellet. Prior to measuring the physico-chemical properties and CO adsorption properties of the thus synthesized CuCl/bayerite pellet (see Section 3.3), we confirmed the transformation of the cellulose derivatives at 573 K, which is the temperature for the TMD step of CuCl. Fig. 2 shows TG/DTG curves of MC, CMC, PMC, HMC, and starch, which were measured while heating the cellulose derivatives to 573 K under a nitrogen flow. All the cellulose derivatives exhibited a two-step weight loss tendency: the first weight loss at temperature lower than 373 K and the second steep weight loss at temperature higher than 473 K. These TG/DTG curves show a similar pattern to those of previously reported typical carbon-based additives [34-38]. Below 473 K, MC, PMC, HMC, CMC, and starch lost 1.8%, 1%, 1%, 3.5%, and 5% of initial weight, respectively, due to dehydration from the cellulose species. Above 473 K, the five celluloses further lost weight via depolymerization, fragmentation, degradation, and carbonization [38-41]. After heating from 473 K to 573 K, and maintaining the final temperature for 8 h, MC, PMC, and HMC retained 15% of carbon residues. CMC and starch retained larger amounts of carbon residues: 45% and 37%, respectively. The carbon residues derived from the cellulose derivatives appear black after the TG/DTG analyses. This indicates that the cellulose-type organic binder might be transformed to carbon residue while making the CuCl/bayerite pellet, and a small amount of

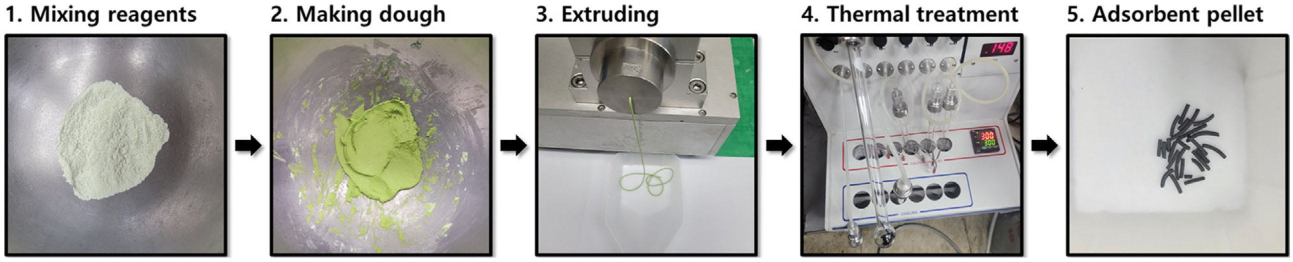

Fig. 1. Process of the preparation of CuCl/bayerite pellet using cellulose derivatives as binder species.

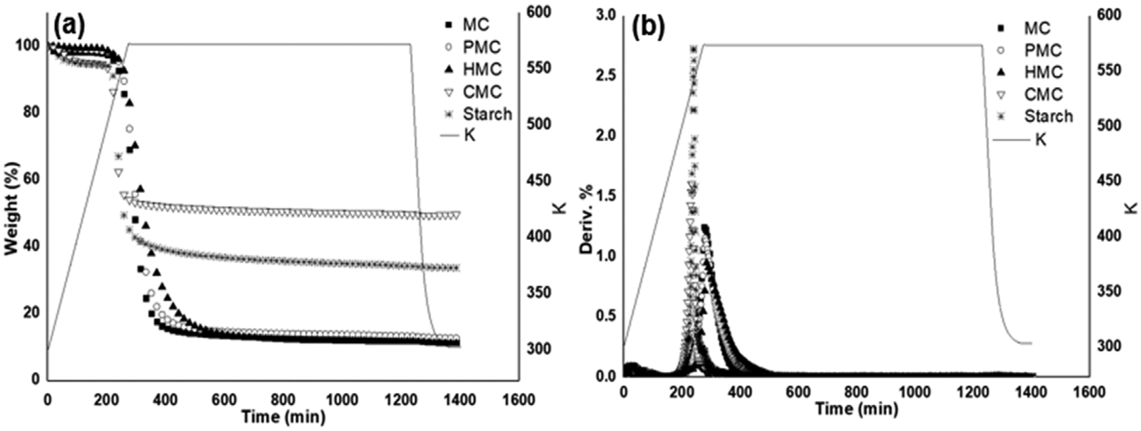

Fig. 2. (a) TG and (b) DTG curves of MC, PMC, HMC, CMC and starch taken while heating to 573 K under nitrogen flow.

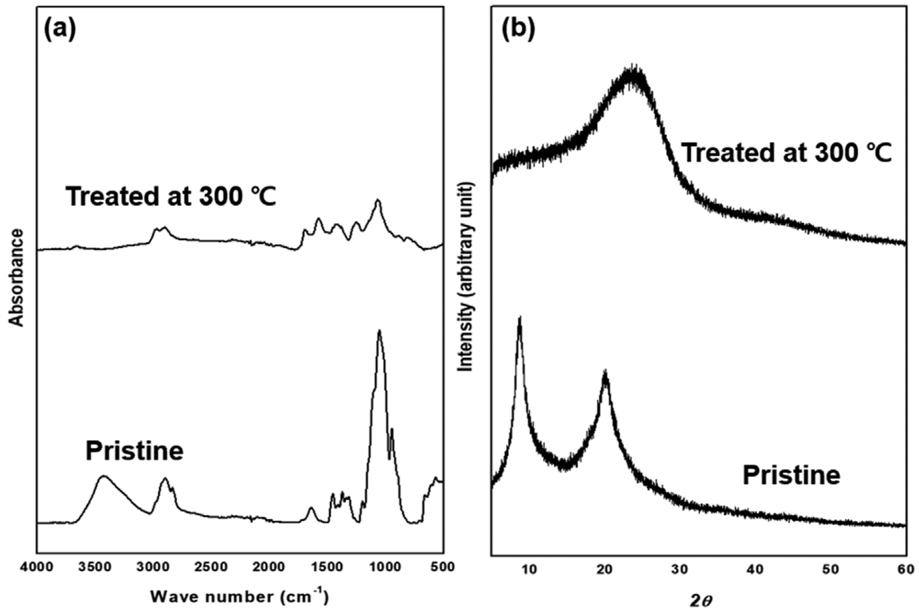

Fig. 3. (a) FT-IR spectra and (b) XRD patterns of pristine MC and carbon residue derived from MC through heat treatment at 573 K under nitrogen flow.

carbon residue is still present in the CuCl/bayerite pellet, maintaining the pellet shape of the adsorbent as a binder species. Notably, the CuCl/bayerite pellet appears blackish after the TMD process.

To understand the transformation of cellulose derivatives at high temperature, molecular structures of the carbon residues derived from MC were characterized by FT-IR and XRD analyses. Fig. 3(a) shows the FT-IR spectra of pristine MC and carbon residue derived from MC by heating at 573 K. The pristine MC shows a strong IR peak in the ranges of 1,300-800 cm^{-1} and 4,000-3,400 cm^{-1}: the former corresponding to C-O-C/C-O stretching and the latter corresponding to O-H stretching. These strong peaks of the pristine MC are ascribed to the presence of hydroxyl groups and ether groups in cellulose monomer. However, after heat treatment at 573 K, these peaks disappeared significantly, while peaks in the range of 1,600-1,400 cm^{-1} (C=C stretching) became larger. This indicates that the pristine cellulose was fully dehydrated and many glycoside bonds in the cellulose were broken at 573 K [41-45]. Meanwhile, the cellulose species transformed to char-type carbon residue containing sp^2 carbon (C=C bond).

Fig. 3(b) shows XRD patterns of the pristine MC and the carbon residue derived from MC by heating at 573 K. The pristine MC shows two strong and sharp peaks centered at 7.5° and 20° of two theta, and this pattern corresponds to the typical XRD pattern of MC [41,42]. This result means that the pristine MC has a somewhat ordered structure. However, after heat treatment at 573 K, these peaks almost fully disappeared, while a broad peak centered at 22.5° (corresponding to amorphous carbon species) appeared. This result indicates that the MC species loses its partially ordered structure during the heat treatment at 573 K.

3. Physico-chemical Properties and CO Adsorption Properties of CuCl/Bayerite Pellet

To synthesize a CuCl/bayerite pellet, we used activated bayerite

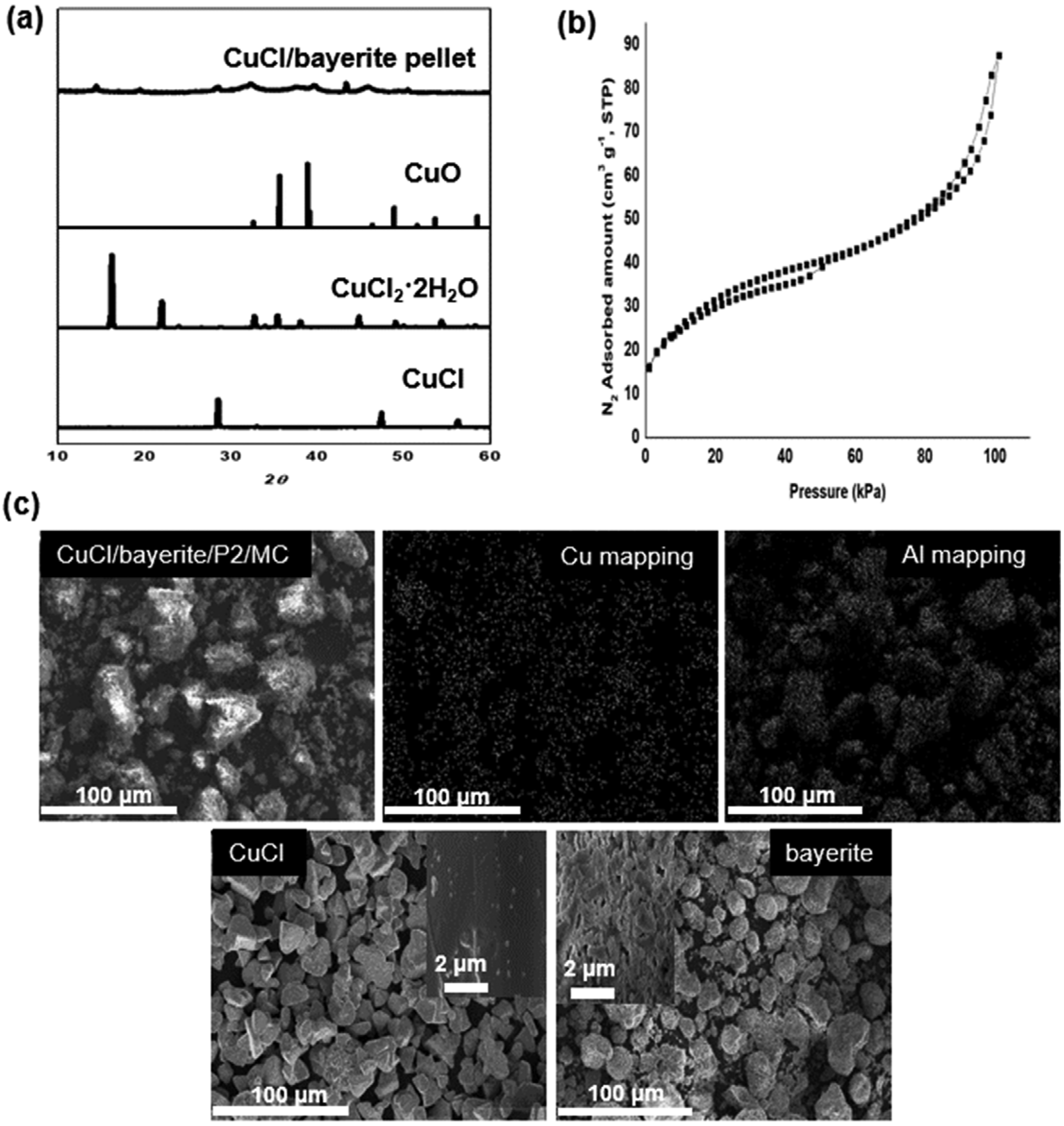

Fig. 4. (a) XRD pattern, (b) N_2 sorption isotherm (taken at 77 K), and (c) SEM/EDS images of CuCl/bayerite pellet.

that was prepared via calcination of a pristine bayerite material at 573 K, because the BET external surface area of the bayerite increases significantly as transformed to η- and θ-phase alumina species via the activation process [22]. The weight ratio of CuCl to bayerite was fixed at 3.6/6.4, and the TMD temperature was fixed at 573 K. The type of cellulose derivatives and the amount of the cellulose derivatives were varied to optimize the synthesis conditions of the CuCl/bayerite pellet. However, most physico-chemical characterizations for the CuCl/bayerite pellet such as BET measurement, XRD measurement, SEM/EDS analysis, and mechanical strength measurement were performed for a standard sample (bayerite : CuCl : inorganic binder, MC=6.4 : 3.6 : 1 : 1 in weight ratio), in comparison with previous characterization results of a CuCl/bayerite powder sample reported in our previous work [22].

Fig. 4(a) shows XRD patterns of the thus synthesized CuCl/bayerite pellet and activated bayerite. The CuCl/bayerite pellet sample shows small and broad XRD peaks centered at 14°, 19°, 28°, 38°, and 46° of 2 theta, and these peaks are representative XRD peaks of activated bayerite material. No XRD peak for CuCl, $CuCl_2$, or CuO species appeared. This result demonstrates that CuCl was highly dispersed on the activated bayerite material with very small particle size and the pristine CuCl species was not oxidized during the synthesis of the CuCl/bayerite pellet. High dispersion of CuCl on the bayerite material was also confirmed by SEM/EDS measurement (see Fig. 4(c)). An SEM image of the CuCl/bayerite pellet shows agglomerates of round-shaped particles with similar particle morphology to that of bayerite particles. No distinct particle with a typical morphology of CuCl crystals was observed. An EDS elemental mapping image of the sample verifies that Cu element from CuCl and Al element from bayerite are well dispersed in the entire range of the adsorbent particles. The CuCl species might be well dispersed as the CuCl/bayerite powder sample was prepared previously, although MC was added in this work to pelletize the CuCl/bayerite adsorbent.

The porous texture of the CuCl/bayerite pellet was characterized by N_2 sorption analysis. Fig. 4(b) shows the N_2 sorption iso-

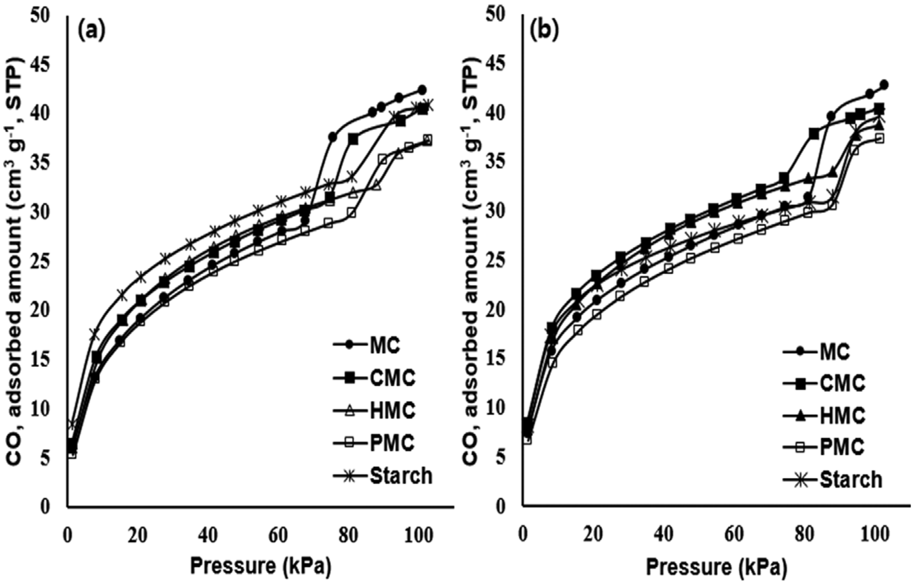

Fig. 5. CO adsorption isotherms (taken at 293 K) of CuCl/bayerite pellet samples synthesized using various types of cellulose derivatives: (a) fresh samples, and (b) samples exposed to humid air-condition for seven days.

Table 1. CO adsorption capacity of various CuCl/bayerite pellet samples and $CuCl_2$/bayerite pellet sample

Composition (in weight ratio)	Adsorbed amount of CO(cm^3/g)	
	Pristine	After 7 days of exposure to humid air-condition
6.4 bayerite : 3.6 CuCl: inorganic binder: 0.2 MC	48.8	9.6
6.4 bayerite : 3.6 CuCl: inorganic binder: 0.6 MC	46.9	34.4
6.4 bayerite : 3.6 CuCl: inorganic binder: 1 MC	42.4	42.7
6.4 bayerite : 3.6 CuCl: inorganic binder: 1.4 MC	32.2	33.2
6.4 bayerite : 3.6 CuCl: inorganic binder: 1 CMC	40.5	40.4
6.4 bayerite : 3.6 CuCl: inorganic binder: 1 HMC	37.3	38.7
6.4 bayerite : 3.6 CuCl: inorganic binder: 1 PMC	37.2	37.3
6.4 bayerite : 3.6 CuCl: inorganic binder: 1 Starch	40.9	39.6
6.4 bayerite: 3.6 $CuCl_2 \cdot 2H_2O$: inorganic binder: 1 MC	31.6	31.4

therm of the CuCl/bayerite pellet measured at 77 K, and the isotherm has a type-IV curve shape, which is a typical shape of a mesoporous material. The BET surface area and total pore volume of the CuCl/bayerite pellet were 129 m^2 g^{-1} and 0.14 cm^3 g^{-1}, respectively. These values are much smaller than the BET surface area and the total pore volume of CuCl/bayerite powder (see Ref. [22]). This result indicates that the addition of binder species partially blocked the pore structure of the CuCl/bayerite particles.

Nevertheless, thus synthesized CuCl/bayerite pellet shows a similar CO adsorption capacity to that of CuCl/bayerite powder. Fig. 5(a) shows CO adsorption isotherms (taken at 293 K) of a series of CuCl/bayerite pellet samples synthesized using the same amounts of different types of cellulose derivatives (MC, CMC, HMC, PMC, and starch). The adsorption amounts of CO under 101 kPa of CO gas at 293 K were measured for all the samples, and the values are provided in Table 1. All the adsorbent pellets show similar curve shapes of CO adsorption isotherms. The CO adsorption capacity was the smallest (37.2 cm^3 g^{-1}) when PMC was used as the binder species, but this value is quite high compared to previous CO adsorbents reported elsewhere [21,23,46]. CO adsorption capacity of 42.4 cm^3 g^{-1} was achieved when MC was used as the binder species. According to a previous report, 30 wt% CuCl/bayerite powder (no addition of MC) and 36 wt% CuCl/bayerite samples exhibited CO adsorption capacities of 48.5 cm^3 g^{-1} and 41.6 cm^3 g^{-1}, respectively. In the case of the present CuCl/bayerite pellet sample, the CuCl content was calculated to be 32 wt% relative to the entire adsorbent considering the amount of carbon residues derived from the MC binder and the amount of inorganic binder additive. Considering this CuCl content, the CO adsorption capacity (42.4 cm^3 g^{-1}) appears to be a reasonable value as compared to the previous CuCl/bayerite powder samples, and the addition of MC does not allow a decrease of CO adsorption capacity.

The CuCl/bayerite pellet also exhibited high CO selectivity to CO_2, H_2, N_2, and CH_4 species, on par with the CuCl/bayerite pow-

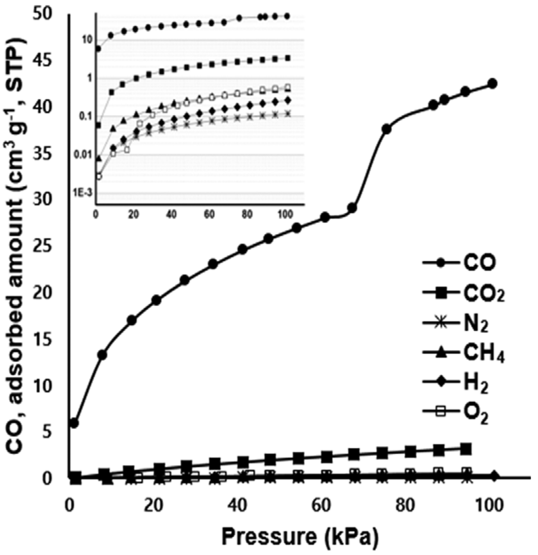

Fig. 6. Sorption isotherms (taken at 293 K) of CuCl/bayerite pellet synthesized using MC (6.4 Bayerite: 3.6 CuCl: 1 MC) for CO, CO_2, N_2, CH_4, H_2, and O_2. The sorption isotherms were also plotted in logarithm scale, and included as an inset of this figure.

der. Fig. 6 shows adsorption isotherms of the CuCl/bayerite pellet sample for CO, CO_2, H_2, N_2, and CH_4 species, and they reveal that the CuCl/bayerite pellet sample exhibited very small adsorption capacity for all the species except for CO. The CuCl/bayerite pellet shows separation factors of 12.6 for CO/CO_2, 352 for CO/N_2, 81 for CO/CH_4, and 162 for CO/H_2. For comparison, according to a previous paper [22], CuCl/bayerite powder shows separation factors of 16.8 for CO/CO_2, 542 for CO/N_2, 187 for CO/CH_4, and 48.9 for CO/H_2. Although the CuCl/bayerite pellet shows somewhat smaller CO selectivity to all other impurities except for H_2 than the powder form, the separation factor values are still remarkably high in terms of application of this adsorbent pellet for separation of CO from other impurities.

To assess the possibility of this CuCl/bayerite in application to a commercialized separation process, we evaluated two important requirements of the adsorbent: mechanical strength and recyclability of the adsorbent from the viewpoint of CO adsorption. We used a hardness measuring instrument (IMADA, Digital Force Gauge Push-Pull DPS-20R) to measure the mechanical strength of the CuCl/bayerite pellet, and the resultant mechanical strength was averaged from ten measurements. The CuCl/bayerite pellet shows mechanical strength of 1.3 kg_f, and this mechanical strength is sufficiently high, as considering that typical zeolite-type commercial adsorbents show mechanical strength of approximately 1.0 kg_f. To assess the recyclability of the CuCl/bayerite pellet, we repeated measurements of the CO adsorption isotherms at 293 K three times. Between each measurement, the adsorbent pellet was evacuated at 573 K for 6 h to desorb the adsorbed CO molecules. Fig. 7 shows the results of the recyclability test, exhibiting that the CuCl/bayerite pellet has the same CO adsorption capacity after the evacuation/regeneration treatment at 573 K. This means that the adsorbent pellet can be completely regenerated by simple evacuation treatment.

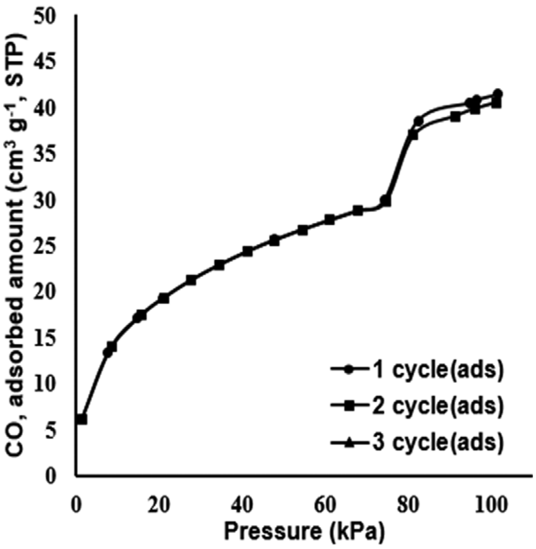

Fig. 7. CO sorption isotherms (taken at 293 K) of CuCl/bayerite pellet sample synthesized using MC (6.4 Bayerite: 3.6 CuCl: 1 MC), measured three times with including a regeneration step (at 573 k under vacuum for 6 h) in between each measurement.

4. Long-term Resistance of CuCl/Bayerite Pellet Against Oxidation

The present CuCl/bayerite-type CO-selective adsorbent was prepared by dispersing CuCl species that show strong interaction with CO molecules on activated bayerite. It is well known that the Cu^+ cations in CuCl are easily oxidized to Cu^{2+} and lose their CO adsorption ability [30-32]. In our preliminary study to prepare a CuCl/bayerite pellet, interestingly we confirmed that CuCl species appear to be rarely oxidized. In addition, the CuCl/bayerite-pellet still shows similar CO adsorption capacity to the initial CO adsorption capacity of the fresh sample after exposing the adsorbent to the atmosphere for several days. In contrast, the CuCl/bayerite powder adsorbent that was synthesized without adding MC species was easily oxidized after exposure for just a few days. The color of the powder adsorbent changed to green, which means the CuCl species is oxidized, and the powder adsorbent exhibited significantly reduced CO adsorption capacity. We assumed that the MC species used to make the adsorbent pellet was transformed to char-type carbon residue during the TMD process and it has a special function of restricting the oxidation of CuCl species.

To confirm the anti-oxidation function of carbon residue derived from the MC organic binder, we prepared a series of CuCl/bayerite pellet adsorbents by using different amounts of MC organic binder (bayerite : CuCl : MC=6.4 : 3.6 : 0.2, 0.6, 1 or 1.4, in weight ratio). We measured CO adsorption isotherms of fresh samples of the adsorbents at 293 K, and the isotherms are shown in Fig. 8(a). After the isotherm measurements, the adsorbent samples were exposed to a humid air condition at room temperature for seven days, and then CO adsorption isotherms were measured again for the adsorbent samples (see Fig. 8(b)). The amounts of CO adsorption for both fresh and exposed adsorbent samples were measured under 101 kPa at 293 K, and these values are provided in

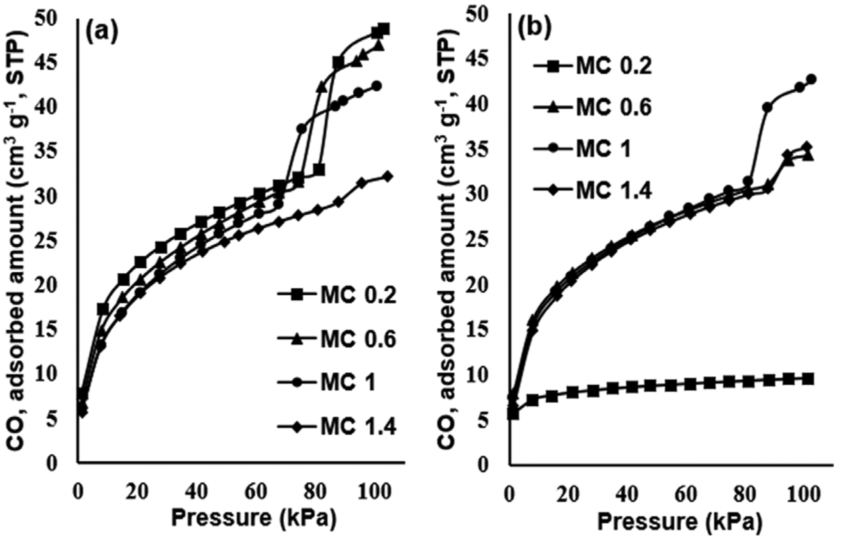

Fig. 8. CO adsorption isotherms (taken at 293 K) of CuCl/bayerite pellet samples synthesized using different amount of MC: (a) fresh samples, and (b) samples exposed to humid air-condition for seven days.

Table 1. As shown in Fig. 8 and Table 1, the CO adsorption amount of fresh adsorbent gradually decreased from 48.8 cm^3 g^{-1} to 32.2 cm^3 g^{-1} as the ratio of MC was increased from 0.2 to 1.4. This tendency is sufficiently predictable, because the ratio of CuCl species to entire adsorbent decreases with an increase of the MC content. After seven days of exposure, the CO adsorption capacity of the adsorbents changed dramatically. When 0.2 MC (smallest amount of MC addition) was used to make the CuCl/bayerite pellet, the CO adsorption amount was reduced from 48.8 cm^3 g^{-1} (fresh sample) to 9.6 cm^3 g^{-1} after seven days of exposure. This result means that the adsorbent was oxidized quite significantly and lost 80% of its initial CO adsorption capacity. When 0.6 MC was used, the CO adsorption amount was reduced from 46.9 cm^3 g^{-1} to 34.4 cm^3 g^{-1}. In this case, the rate of decrease of CO adsorption capacity due to the exposure was 27% and this value was much smaller than the case of using 0.2 MC. The use of 0.2 or 0.6 MC appears to be insufficient to maintain the oxidation state of the CuCl and initial CO adsorption capacity. In contrast, the adsorbent samples synthesized using a larger amount of MC (*i.e.*, 1.0 MC and 1.4 MC) completely maintained the initial CO adsorption capacity even after seven days of exposure. More notably, the CuCl/bayerite pellet adsorbent synthesized from the precursor mixture with a weight ratio of 6.4 bayerite: 3.6 CuCl: 1.0 MC maintains 90% of the initial CO adsorption capacity after 100 days of exposure.

In this systematic study, it is determined that the carbon residue derived from the MC organic binder has a strong function to resist the oxidation of CuCl species in the pellet adsorbent under a humid air condition. In addition, the use of MC with at least a 1.0/10 MC/(CuCl+bayerite) weight ratio is necessary to maintain the oxidation state of the CuCl and the initial CO adsorption capacity. When other cellulose derivatives such as CMC, HMC, PMC, and starch were used as binder species with a 1.0/10 MC/(CuCl+bayerite) weight ratio, we confirmed that the initial CO adsorption capacity can be completely maintained after seven days of exposure (see Fig. 5(b) and Table 1).

5. Reducing role of Methyl Cellulose to CuCl/Bayerite Pellet

It is noteworthy that the use of cellulose allows pelletization of the CuCl/bayerite adsorbent (role of main binder species) and simultaneously prevents the oxidation of CuCl species in the adsorbent (role of anti-oxidation agent or reducing agent). It is clear that the use of cellulose derivatives species is effective to maintain the CO adsorption capacity, according to the comparative measurements of CO adsorption isotherms for the fresh CuCl/bayerite pellet adsorbent and the adsorbent sample exposed to a humid air condition for seven days. However, the results do not provide direct evidence to clarify the exact role of carbon residue derived from the cellulose species to the CuCl/bayerite pellet. We propose two possible mechanisms whereby the carbon residue could retain the CO adsorption capacity: 1) the carbon residue physically interrupts the adsorption of oxygen species, which is a strong oxidizing agent to the CuCl species, without any reactant role, or 2) the carbon residue continuously reduces the oxidized state of CuCl species to recover the strong CO adsorption ability.

To confirm the possibility of the first mechanism, we comparatively measured oxygen adsorption isotherms at 293 K for both CuCl/bayerite adsorbents in powder form (synthesized without adding MC) and in pellet form (synthesized with MC). Fig. 9 presents the oxygen adsorption isotherms of the two adsorbent samples, which show almost the same oxygen adsorption capacity. Both adsorbent samples adsorbed a very small amount of oxygen at 293 K. The addition of MC appears to have no specific effect to interrupt the adsorption of oxygen species to CuCl species.

To confirm the possibility of the second mechanism, we applied MC to the $CuCl_2$/bayerite-based adsorbent. A $CuCl_2$/bayerite adsorbent was synthesized via the same route as employed for CuCl/bayerite, except for using $CuCl_2 \cdot 2H_2O$ instead of CuCl. $CuCl_2$ is a further oxidized form of CuCl, and it is known to have no strong interaction with CO molecules, in contrast to CuCl [30-32]. Nevertheless, $CuCl_2$ (especially hydrated form) is highly water-soluble and inexpensive, and as such has been used to synthesize CO-

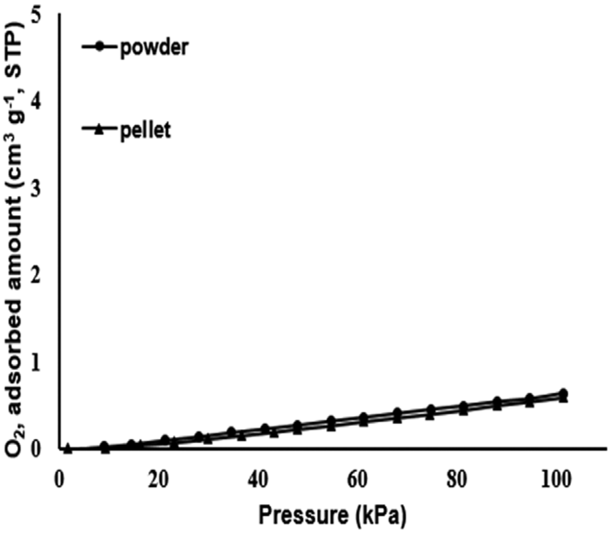

Fig. 9. O_2 sorption isotherms (taken at 293 K) of CuCl/bayerite powder sample (without using MC) and pellet sample (with using MC).

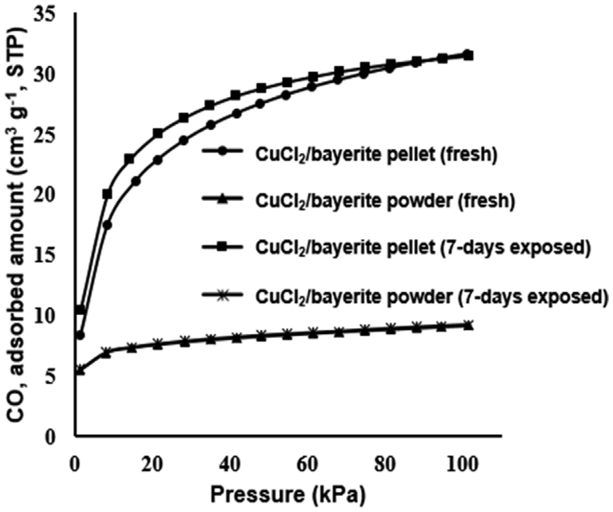

Fig. 11. CO adsorption isotherms (taken at 293 K) of $CuCl_2$/bayerite powder sample and pellet sample, as pristine and as exposed to humid air-condition for seven days.

selective adsorbents [47-49]. The $CuCl_2$ species can be well dispersed on nanoporous supporting materials via simple wetness impregnation, but it should be reduced to Cu^+ species that strongly interact with CO molecules.

Fig. 10 shows XPS spectra and XRD patterns of $CuCl_2$/bayerite samples that were thermally treated at 573 K under a vacuum condition, with the addition of MC and without MC. For comparison, XPS spectra and XRD patterns of CuCl and $CuCl_2 \cdot 2H_2O$ were also provided. As shown in Fig. 10, $CuCl_2$/bayerite powder sample synthesized without MC shows XPS peaks corresponding to Cu^{2+} species, centered at binding energy of 963 eV, 952 eV, 942 eV, and 932 eV and a sharp and strong XRD peak corresponding to $CuCl_2$ species, centered at 16° of two theta. Meanwhile, this sample exhibited no distinct XPS or XRD peaks of Cu^+ species. This indicates that the $CuCl_2$/bayerite powder sample still has Cu^{2+} species after thermal treatment. On the other hand, the $CuCl_2$/bayerite pellet sample that was synthesized using MC binder species via thermal treatment shows strong XPS peaks corresponding to Cu^+ species, centered at 951 eV and 931 eV, and a tiny (due to high dispersion of Cu^+ species) XRD peak for CuCl, centered at 27°, and it does not show any distinct XPS or XRD peaks of Cu^{2+} species. Moreover, this $CuCl_2$/bayerite pellet sample shows the same XPS spectrum after seven days of exposure of the sample to a humid air condition, indicating that Cu^+ species in this sample retains its oxidation state. It is interesting that the Cu^{2+} species in the $CuCl_2$/bayerite mixture was completely converted to Cu^+ species through thermal treatment at 573 K in the presence of MC

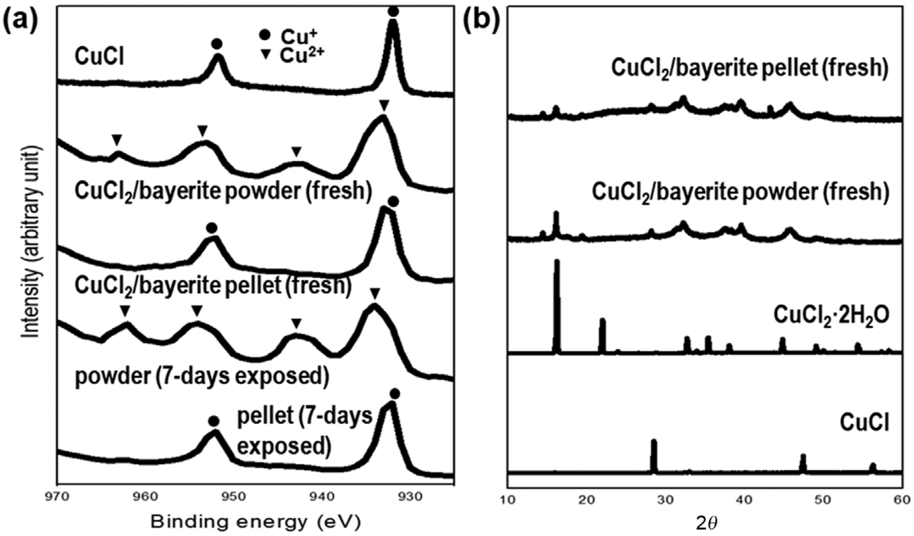

Fig. 10. (a) XPS spectra and (b) XRD patterns of $CuCl_2$/bayerite powder samples (prepared without using MC) and pellet samples (with using MC).

species and the oxidation state was not returned to Cu^{2+} by exposure to air.

CO adsorption isotherms of these $CuCl_2$/bayerite powder and $CuCl_2$/bayerite pellet samples show consistent results with those of the XPS and XRD analyses. As shown in Fig. 11, the $CuCl_2$/bayerite powder sample exhibited small CO adsorption capacity (10 $cm^3\ g^{-1}$ under 101 kPa at 293 K), as compared to the CuCl/bayerite pellet samples. This is because the $CuCl_2$/bayerite mostly has Cu^{2+} species showing no specific interaction with CO molecules (see also Fig. 10). However, the $CuCl_2$/bayerite pellet sample synthesized with MC exhibited high CO adsorption capacity (31.6 $cm^3\ g^{-1}$ under 101 kPa at 293 K). Considering that the same weight of CuCl and $CuCl_2{\cdot}2H_2O$ was used to synthesize the CuCl/bayerite pellet and $CuCl_2$/bayerite pellet samples, respectively (that is, the $CuCl_2$/bayerite pellet sample has a smaller amount of Cu species than the CuCl/bayerite pellet), the $CuCl_2$/bayerite pellet sample appears to show comparable CO adsorption capacity to the CuCl/bayerite pellet sample. In addition, the $CuCl_2$/bayerite pellet sample can closely maintain the initial CO adsorption capacity even after seven days of exposure of the sample to a humid air condition (see Fig. 11).

According to the above results of XPS, XRD, and CO adsorption measurements, our second proposed mechanism of MC species is feasible. The MC species transformed to carbon residue during thermal treatment, and we confirmed that the carbon residue has sufficiently strong reducing power to convert Cu^{2+} to Cu^+. As well as the $CuCl_2$/bayerite pellet sample, the carbon residue is expected to retain the oxidation state of Cu^+ species in the CuCl/bayerite pellet sample by its reducing role. The reducing role of carbon species in various industrial fields was reported in a few previous papers [50-52]. The use of MC enables pelletization of the CuCl/bayerite adsorbent and protects the CuCl species against oxidation, and it is also meaningful that the use of MC enables the synthesis of a readily CO-selective adsorbent using a $CuCl_2$ component. As mentioned above, $CuCl_2$ is highly water-soluble and inexpensive, while affording an easy preparation method (simple wetness impregnation instead of TMD) and low production cost of CuCl in the preparation of a CuCl-based CO adsorbent. However, it is necessary to reduce $CuCl_2$ to CuCl via an additional treatment step, before its use in CO adsorption, and it is difficult to reduce selectively Cu^{2+} to Cu^+ without generating the fully reduced Cu(0) metallic state. In this work, we demonstrated that it is possible to synthesize a readily CO-selective adsorbent using $CuCl_2$ with MC, without an additional reduction treatment, and thus the synthesized adsorbent shows sufficiently high CO adsorption capacity.

CONCLUSION

For application of this adsorbent in the real field of adsorption/separation processes, we synthesized a CuCl/bayerite pellet using a cellulose derivative binder and an inorganic binder additive. Various types of cellulose derivatives such as MC, CMC, HMC, PMC, and starch with varied amounts were tested to find the best organic binder to make a CuCl/bayerite pellet showing high mechanical strength and high CO adsorption properties. We confirmed that the CuCl/bayerite pellet can be synthesized with high mechanical strength (1.3 kg_f) sufficient for use in separation processes, and this adsorbent pellet still shows high CO adsorption capacity (42.4 $cm^3\ g^{-1}$) and high CO selectivity against other components (separation factors of 12.6 for CO/CO_2, 352 for CO/N_2, 81 for CO/CH_4, and 162 for CO/H_2), when MC is used as the binder species. The MC binder species was carbonized and converted to carbon residue during the TMD step, and this carbon residue might retain the shape of the adsorbent pellet.

More notably, we discovered that the carbon residue derived from the MC binder species has another critical role in the CuCl/bayerite pellet adsorbent of serving as a reducing agent for CuCl species. The CuCl/bayerite pellet adsorbent that was synthesized using MC species completely retained the initial CO adsorption capacity even after seven days of exposure of the adsorbent to a humid air condition (retaining 90% of CO adsorption capacity for 100 days), while the CuCl/bayerite powder adsorbent synthesized without using MC species significantly lost CO adsorption ability in just a few days of exposure. We confirmed that the carbon residue has strong reducing power sufficient for reducing Cu^{2+} to Cu^+ at 573 K. Because of the dual function of MC (binder species and reducing agent), it is possible to synthesize a CuCl/bayerite-based CO adsorbent in pellet form that shows high CO adsorption capacity, CO selectivity, and longevity via a simple method. In addition, the use of MC allows the synthesis of a CO adsorbent using $CuCl_2$ species, which is much cheaper and easier to be impregnated than CuCl, without an additional complicated reduction process to convert $CuCl_2$ to Cu(I) species. The present CuCl/bayerite adsorbent in pellet form can be used in CO-separation processes in various CO-generating fields such as the steel-making industry, steam-methane-reforming (SMR) processes, and partial-oxidation (POX) processes.

ACKNOWLEDGEMENTS

This work was conducted under the framework of Research and Development Program of the Korea Institute of Energy Research (KIER, C1-2433).

REFERENCES

1. S. Mahajan and S. Jagtap, *Mater. Today*, **18**, 100483 (2020).
2. Y. ding and E. Alpay, *Chem. Eng. Sci.*, **55**, 3929 (2000).
3. Å. Slagtern and U. Olsbye, *Appl. Catal.*, **110**, 99 (1994).
4. S. A. Bhat and J. Sadhukhan, *AIChE J.*, **55**, 408 (2009).
5. S. S. Hou, C. H. Chen, C. Y. Chang, C. W. Wu, J. J. Ou and T. H. Lin, *Energy Convers. Manage.*, **52**, 2758 (2011).
6. G. Zarca, I. Ortiz and A. Urtiaga, *J. Membr. Sci.*, **438**, 38 (2013).
7. Y. Wang, C. Li, F. Meng, S. Lv, J. Guo, X. Liu, C. Wang and Z. Ma, *Chem. Sci. Eng.*, **8**, 340 (2014).
8. N. Dutta and G. Patil, *Sep. Purif.*, **9**, 277 (1995).
9. H. Tamon, K. Kitamura and M. Okazaki, *AIChE J.*, **42**, 422 (1996).
10. G. Patil, S. Baruah and N. Dutta, *Gas Sep. Purif.*, **5**, 2 (1991).
11. G. S. Soave, S. Gamba and L. A. Pellegrini, *Ind. Eng. Chem. Res.*, **45**, 5761 (2006).
12. F. Kasuya and T. Tsuji, *Gas Sep. Purif.*, **5**, 242 (1991).
13. C. Xue, W. Hao, W. Cheng, J. Ma and R. Li, *Chem. Eng. J.*, **375**, 122049 (2019).

14. J. Peng, S. Xian, J. Xiao, Y. Huang, Q. Xia, H. Wang and Z. Li, *Chem. Eng. J.*, **270**, 282 (2015).
15. N. A. Khan and S. H. Jhung, *J. Hazard. Mater.*, **325**, 198 (2017).
16. J. W. Yoon, T.-U. Yoon, E.-J. Kim, A.-R. Kim, T.-S. Jung, S.-S. Han and Y.-S. Bae, *J. Hazard. Mater.*, **341**, 321 (2018).
17. V. N. Le, T. K. Vo, J. H. Lee, J. C. Kim, T.-H. Kim, K. H. Oh, Y.-S. Bae, S. K. Kwak and J. Kim, *Chem. Eng. J.*, **404**, 126492 (2021).
18. T.-U. Yoon, M. J. Kim, A.-R. Kim, J. H. Kang, D. Ji and Y.-S. Bae, *J. Ind. Eng. Chem.*, **87**, 102 (2020).
19. T. K. Vo, Y.-S. Bae, B.-J. Chang, S.-Y. Moon, J.-H. Kim and J. Kim, *Micropor. Mesopor. Mater.*, **274**, 17 (2019).
20. Y. Xie, J. Zhang, J. Qiu, X. Tong, J. Fu, G. Yang, H. Yan and Y. Tang, *Adsorption*, **3**, 27 (1997).
21. K. Cho, J. Kim, H. T. Beum, T. Jung and S. S. Han, *J. Hazard. Mater.*, **344**, 857 (2018).
22. K. Cho, J. Kim, J.-H. Park, T. Jung, H. T. Beum, D.-W. Cho, Y.-W. Rhee and S. S. Han, *Micropor. Mesopor. Mater.*, **277**, 124 (2019).
23. D. Saha and S. Deng, *J. Chem. Eng. Data*, **54**, 2245 (2009).
24. H. Hirai, K. Wada and M. Komiyama, *Bull. Chem. Soc. Jpn.*, **59**, 2217 (1986).
25. D. H. Gallaba, J. Villarroel-Rocha, K. Sapag and A. d. Migone, *Micropor. Mesopor. Mater.*, **265**, 227 (2018).
26. Y. Wang, R. T. Yang and J. M. Heinzel, *Chem. Eng. Sci.*, **63**, 356 (2008).
27. Y. Huang, Y. Tao, L. He, Y. Duan, J. Xiao and Z. Li, *Adsorption*, **21**, 373 (2015).
28. Y. Wang and Y. Lin, *J. Sol-Gel Sci. Technol.*, **11**, 185 (1998).
29. Y. Yin, P. Tan, X.-Q. Liu, J. Zhu and L.-B. Sun, *J. Mater. Chem. A*, **2**, 3399 (2014).
30. K. Hadjiivanov and H. Knözinger, *Phys. Chem. Chem. Phys.*, **3**, 1132 (2001).
31. K. H. Huang, *J. Mol. Catal.*, **64**, 85 (1991).
32. K. I. Hadjiivanov, M. M. Kantcheva and D. G. Klissurski, *J. Chem.*, **92**, 4595 (1996).
33. M. Jin, S. S. Kim, Y. D. Kim, J.-N. Park, J. H. Kim, C. H. Ko, J.-N. Kim and J. M. Kim, *J. Mater.*, **1**, 6653 (2013).
34. J. Xue, S. Ceylan and J. L. Goldfarb, *Thermochim. Acta*, **618**, 36 (2015).
35. M. Akram, I. Taha and M. M. Ghobashy, *Cellulose*, **23**, 1713 (2016).
36. P. Aggarwal and D. Dollimore, *Talanta*, **43**, 1527 (1996).
37. Z. Wu, S. Wang, J. Zhao, L. Chen and H. Meng, *Fuel*, **171**, 65 (2016).
38. J. B. Wooten, J. I. Seeman and M. R. Hajaligol, *Energy Fuels*, **18**, 1 (2004).
39. W. S.-L. Mok and M. J. Antal, *Thermochim. Acta*, **68**, 165 (1983).
40. F.-X. Collard and J. Blin, *Renewable Sustainable Energy Rev.*, **38**, 594 (2014).
41. C. Zhang, L. Chao, Z. Zhang, L. Zhang, Q. Li, H. Fan, S. Zhang, Q. Liu, Y. Qiao, Y. Tian, Y. Wang and X. Hu, *Renewable Sustainable Energy Rev.*, **135**, 110416 (2021).
42. S. Xin, H. Yang, Y. Chen, M. Yang, L. Chen, X. Wang and H. Chen, *J. Anal. Appl. Pyrolysis*, **116**, 263 (2015).
43. Z. Yang, X. Liu, Z. Yang, G. Zhuang, Z. Bai, H. Zhang and Y. Guo, *J. Anal. Appl. Pyrolysis*, **102**, 83 (2013).
44. H. Yang, R. Yan, H. Chen, D. H. Lee and C. Zheng, *Fuel*, **86**, 1781 (2007).
45. X. Yang, Y. Zhao, R. Li, Y. Wu and M. Yang, *Thermochim. Acta*, **665**, 20 (2018).
46. Y. Wu, Z. Chen, B. Li, J. Xing, H. Liu, Y. Tong, P. Tian, Y. Xu and Z. Liu, *J. Energy*, **36**, 122 (2019).
47. F. Gao and Y. Wang, S. *Chem. Eng. J.*, **290**, 418 (2016).
48. A.-R. Kim, T.-U. Yoon, S.-I. Kim, K. Cho, S.-S. Han and Y.-S. Bae, *Chem. Eng. J.*, **348**, 135 (2018).
49. C. Xue, W. Hao, W. Cheng, J. Ma and R. Li, *Materials*, **12**, 1605 (2019).
50. J. A. Jiménez, *J. Alloys Compd.*, **656**, 685 (2016).
51. L. Klüpfel, M. Keiluweit, M. Kleber and M. Sander, *Environ. Sci. Technol.*, **48**, 5601 (2014).
52. E. H. Hwang, H. G. Seong and S. J. Kim, *Korean J. Met. Mater.*, **56**, 570 (2018).